

# Defect states emerging from a non-Hermitian flat band of photonic zero modes

Li Ge\* and Bingkun Qi

Department of Engineering Science and Physics, College of Staten Island, CUNY, Staten Island, NY 10314, USA and  
The Graduate Center, CUNY, New York, NY 10016, USA

(Dated: April 18, 2017)

In this work we show that there exists a flat band consisting of photonic zero modes in a gain and loss modulated lattice system, as a result of the underlying non-Hermitian particle-hole (NHPH) symmetry. This general finding explains the previous observation in parity-time ( $\mathcal{PT}$ ) symmetric systems where NHPH symmetry is hidden, and it is more general and offers a flexible control of the band structures. We further discuss the defect states in these systems, whose emergence can be viewed as an unconventional alignment of a pseudo-spin under the influence of a complex magnetic field, and in certain cases, the result of a  $\mathcal{PT}$  transition. These defect states also behave as a chain with two types of links, one rigid in a unit cell and one soft between unit cells, as the defect states become increasingly localized with the non-Hermitian parameter.

Defect states are ubiquitous in periodic systems due to the existence of bandgaps. In the simple case of a point defect, if its energy falls deep into a bandgap, then it cannot couple efficiently to the rest of the system, where no propagating mode exists at its energy. As a result, a defect state localized at this point is formed, no matter whether the defect is in the bulk or at the edge of the system. Take the most mundane periodic system in one dimension (1D) for example, its unit cell contains one element of energy  $\omega_0$  that couples to its nearest neighbors with strength  $t > 0$ , where a single band extends from  $[\omega_0 - 2t, \omega_0 + 2t]$  across the Brillouin zone (BZ). A defect state is formed if the on-site energy of a single defect at the edge is detuned from  $\omega_0$  by more than  $t$ , and it appears above (below) this band if the detuning is positive (negative).

A particular interesting case for defect states is in the presence of a flat band, where a small detuning is sufficient to create a defect state in general. A flat band is dispersionless inside the whole BZ, and systems that exhibit flat bands have attracted considerable interest in the past few years, including optical [1, 2] and photonic lattices [3–6], graphene [7, 8], superconductors [9–12], fractional quantum Hall systems [13–15] and exciton-polariton condensates [16, 17]. Due to the singular density of states at the flat band energy, several interesting localization phenomena and their scaling properties have been identified [18–22].

In Refs. [23–25], parity-time ( $\mathcal{PT}$ ) symmetric perturbations, i.e., those with a complex potential satisfying  $V(x) = V^*(-x)$  [26–51], were introduced to study their effects on an existing flat band in the underlying Hermitian system. In the meanwhile, it was known that a  $\mathcal{PT}$ -symmetric potential can collapse two neighboring bands into a single one [32], which is flat in some cases [52, 53]. The conditions that lead to the flatness were poorly understood, and in this work we point out that the mechanism that leads to these flatbands is actually due to another symmetry, i.e., non-Hermitian particle-hole (NHPH) symmetry [54, 55].

With NHPH symmetry, the effective Hamiltonian anti-commutes with an antilinear operator, and a particular simple way to achieve it employs a photonic lattice [55]: starting with an underlying Hermitian system with chiral symmetry (also known as sublattice symmetry), which consists of identical elements on two sublattices coupled by nearest neighbor coupling (e.g., a square lattice, honeycomb lattice and so on), NHPH symmetry is automatically satisfied once spatial gain and loss modulation is applied.

The flat band resulted from NHPH symmetry consists of photonic zero modes, which share certain traits as their condensed matter counterparts (i.e., the Majorana zero modes [56–58]). However, these photonic zero modes are not necessarily localized in space, and we study the defect states emerging from these non-Hermitian flat bands by introducing a point defect. We employ the simplest 1D photonic lattice mentioned before but now with gain and loss modulation that doubles or quadruples the size of the unit cell. We show that a flat band is formed when the gain and loss strength  $\gamma$  exceeds a critical value. Now by introducing a point defect at the edge of the system, a defect state appears and becomes increasingly localized as the non-Hermiticity of the system increases. This defect state behaves as a chain with two types of links, one rigid within a unit cell and one soft between unit cells. We find that the emergence of the defect state can be viewed as an unconventional alignment of a pseudo-spin under the influence of a complex magnetic field, and in some cases, the result of a  $\mathcal{PT}$  transition.

*Non-Hermitian Flat Band* — The periodic system we consider is the simplest 1D lattice mentioned in the introduction, and we choose the identical on-site energy of the lattice sites to the zero point of its energy levels. With the introduction of gain and loss modulation, the non-Hermitian system can be captured by the tight-binding model

$$i\partial_t\psi_n = i\gamma_n\psi_n + t(\psi_{n-1} + \psi_{n+1}) \quad (n = 1, 2, \dots). \quad (1)$$

Below we consider a periodic imaginary potential with  $\gamma_n = \gamma_{n+m}$  where  $m$  is an even integer. For an odd

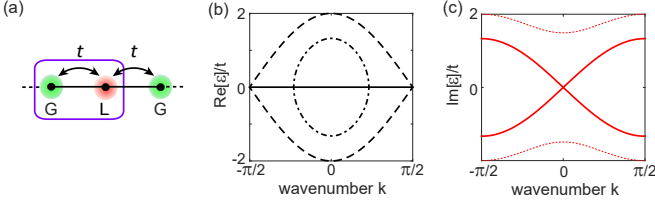


FIG. 1. (Color online) (a) Schematic of a gain and loss modulated lattice with period  $m = 2$ . The box indicates the unit cell. (b) and (c) Real and imaginary parts of the bands in (a). The dashed lines in (b) mark the Hermitian bands when  $\gamma = 0$ . The dash-dotted line show their partial collapse when  $\gamma = 1.5t$ . The solid line shows the completed flat band when  $\gamma \geq 2t$ . The solid and dotted lines in (c) are for  $\gamma = 2t$  and  $3t$ , respectively.

$m$  the system does not have two sublattices and hence NHPH symmetry does not hold. Take  $m = 1$  for example, we have a uniform imaginary potential that simply shifts the energy levels along the imaginary axis, without introducing a flat band or any non-Hermitian effect.

When the period  $m$  equals 2 [see Fig. 1(a)], the effective Hamiltonian can be written in the following form, by dropping an offset of the imaginary potential:

$$H_2 = \begin{bmatrix} i\gamma & t(1 + e^{-2ik}) \\ t(1 + e^{2ik}) & -i\gamma \end{bmatrix}. \quad (2)$$

$\gamma$  here is defined as  $(\gamma_n - \gamma_{n+1})/2$ , and we have set the distance between two neighboring lattice sites to be 1. The dispersion relations of this system are then given by  $\varepsilon_{\pm}(k) = \pm\sqrt{t^2(1 + \cos 2k) - \gamma^2}$  in the BZ  $k \in [-\pi/2, \pi/2]$ . This effective Hamiltonian satisfies

$$\{H_2, \mathcal{CT}\} = 0, [H_2, \mathcal{PT}] = 0, \quad (3)$$

i.e., it has both NHPH symmetry and  $\mathcal{PT}$  symmetry. Here  $\mathcal{T}$  is the time-reversal operator in the form of the complex conjugation, and the chiral operator  $\mathcal{C} = \sigma_z$  and parity operator  $\mathcal{P} = \sigma_x$  are given by the Pauli matrices. The curly and square brackets denote anti-commutation and commutation relations as usual.

We note that  $\mathcal{PT}$  symmetry dictates that the bands of the system satisfy  $\varepsilon_i(k) = \varepsilon_j^*(k)$ . In the case that  $i, j$  are different, the two bands have the same  $\text{Re}[\varepsilon]$  but different  $\text{Im}[\varepsilon]$ , which was a result of spontaneous  $\mathcal{PT}$  symmetry breaking [27]. Nevertheless,  $\mathcal{PT}$  symmetry does not dictate that their identical  $\text{Re}[\varepsilon]$  needs to be flat in the BZ, and in Ref. [32] this merged band was indeed found to be curved.

NHPH symmetry, on the other hand, leads to a band structure satisfying  $\varepsilon_i(k) = -\varepsilon_j^*(k)$  instead [55]. It clearly indicates that when  $i = j$ , a flat band at  $\text{Re}[\varepsilon] = 0$  can emerge with photonic zero modes. For the  $m = 2$  case above, this flat band starts to emerge from the boundary of the BZ as soon as  $\gamma$  is nonzero, and it is formed completely when  $\gamma > \gamma_c \equiv 2t$  [see Fig. 1(b)].

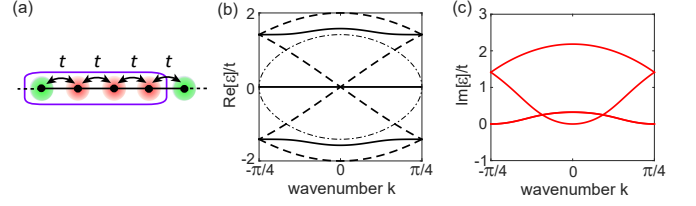


FIG. 2. (Color online) (a) Schematic of a gain and loss modulated lattice with period  $m = 4$ . The box indicates the unit cell. (b) and (c) Real and imaginary parts of the bands in (a) when  $\gamma_a = 2\sqrt{2}t$  (solid lines). The dashed and dash-dotted lines in (b) show the Hermitian bands when  $\gamma_a = 0$  and the case  $\gamma_a = \gamma_c = 2\sqrt{2}t$ , respectively.

Next we take a look at the  $m = 4$  case [see Fig. 2(a)]. The effective Hamiltonian still satisfy NHPH symmetry but not  $\mathcal{PT}$  symmetry in general. It can be written as

$$H_4 = \begin{bmatrix} i\gamma_a & t & 0 & te^{-4ik} \\ t & i\gamma_b & t & 0 \\ 0 & t & i\gamma_c & t \\ te^{4ik} & 0 & t & 0 \end{bmatrix} \quad (4)$$

where  $\gamma_{a,b,c} = \gamma_n - \gamma_{n+1, n+2, n+3}$ . For simplicity, we consider just one nonzero  $\gamma$  (e.g.,  $\gamma_a$ ). As Fig. 2(b) shows,  $\gamma_a$  creates a bandgap between the lower two bands and upper two bands respectively, and it collapses the central two bands into a flat band, starting from the center of the BZ which is completed when  $\gamma_a \geq 2\sqrt{2}t$ , again with photonic zero modes at  $\text{Re}[\varepsilon] = 0$ . The lack of  $\mathcal{PT}$  symmetry is obvious from the imaginary part of the bands shown in Fig. 2(c), which would otherwise have a up-down symmetry. Due to the periodicity of the system, the same results hold if we use  $\gamma_b$  or  $\gamma_c$  as the nonzero non-Hermitian parameter.

Although we do not discuss the case of more than one nonzero  $\gamma$  in detail, we mention that the two bandgaps next to the flat band shrink if we have a finite and positive  $\gamma_c$ , and they close completely when  $\gamma_c = 2\sqrt{2}t$  [see Fig. 2(b)]. This tunability offers a flexible control of the non-Hermitian band structures, which the simple  $\mathcal{PT}$ -symmetric modulation of  $m = 2$  lacks.

**Defect States** — Henceforth we focus on the  $m = 2$  case, as the properties of the defect states in the  $m = 4$  case are similar. The emergence of a defect state is exemplified in Fig. 3(a), when a defect of detuning  $\Delta$  is introduced to the left edge of the system (now of a finite length). We note that the defect state is formed at a small  $\Delta$  as a result of the flat band, which is in contrast to the Hermitian case (e.g., the mundane 1D lattice) we have mentioned in the introduction.

One interesting feature of the defect state is its staggered intensity profile on the log scale [see Figs. 3(c) and (d)]: if we define the unit cells by counting from the  $n = 2$  site (i.e., avoiding the defect at the left edge), the intensity ratio  $R$  within each unit cell is a constant for all unit cells.

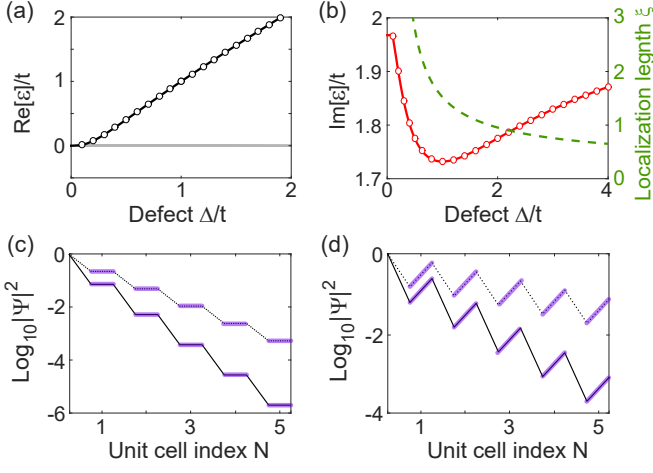


FIG. 3. (Color online) Emergence of a defect state from a non-Hermitian flat band as a function of the defect detuning  $\Delta$ , where the period of the gain and loss modulation is  $m = 2$ . (a) and (b) Real and imaginary parts of the defect state energy as a function of the detuning  $\Delta$ . The solid lines and the dots show numerical results and the analytical expression (5), respectively.  $\gamma = 2t$  is used. In (a) the grey lines show the almost unperturbed flat band energies of the bulk modes. In (b) the dashed line shows the localization length of the defect state. (c) Intensity profile of the defect state with  $\Delta = t$ .  $\gamma = 2t$  (1.3t) for the solid (dotted) line. Only the left 5 unit cells are shown (marked by the “rigid links” that are parallel and  $\gamma$ -independent). (d) Same as (c) but with  $\Delta = t/2$ .  $\gamma = 2t$  (1.1t) for the solid (dotted) line.

The same is true for the intensity ratio  $R'$  between the gain (loss) sites in two neighboring unit cells. Based on these observations, we derive an analytical expression for  $\varepsilon_\Delta$  of the defect state:

$$\varepsilon_\Delta = \frac{(t^2 + \Delta^2) \mp \sqrt{(t^2 - \Delta^2 - 2i\gamma\Delta)^2 + 4t^2\Delta^2}}{2\Delta}, \quad (5)$$

where the “ $-(+)$ ” sign should be used for  $\Delta < t$  ( $\Delta > t$ ). This expression agrees nicely with the numerical data in Figs. 1(a) and (b).

Furthermore, we find that the intra-cell intensity ratio  $R$  mentioned above is simply given by

$$R = \frac{\Delta^2}{t^2} \quad (6)$$

and *independent* of the non-Hermitian parameter  $\gamma$ . In the meanwhile, the inter-cell intensity ratio  $R'$  is given by

$$R' = \frac{\Delta^4}{t^4} \left| \frac{\varepsilon_\Delta + i\gamma}{\varepsilon_\Delta - i\gamma} \right|^2, \quad (7)$$

which does vary with  $\gamma$ . Therefore, the defect state behaves as a chain with two types links as we increase the non-Hermiticity of the system via  $\gamma$ , one rigid within a unit cell and one soft between unit cells. This feature highlights a key contrast between zero modes due to NHPH

symmetry and those due to chiral symmetry (for example, in the Su-Schrieffer-Heeger model [59, 60]): the wave functions of the latter vanish on one sublattice and  $R$  becomes meaningless.

Fixed inter-cell and intra-cell intensity ratios also indicate that the wave function of the defect state is exponentially localized on both sublattices [see Fig. 1(c) and (d)], with the *same* localization length given by  $\xi = 4/\ln R'$ . At first glance this result may seem counterintuitive since one sublattice has gain and the other has loss, but we remind the reader that gain and loss do not describe wave propagation along the lattice. It is most obviously in a photonic lattice made up of parallel waveguides, where the gain and loss characterizes wave propagation *along* the waveguides (i.e., “into the paper”). We also note that the localization length is not directly related to  $\text{Im}[\varepsilon_\Delta]$ . The latter is determined simultaneously by  $R$  and  $R'$ , which lead to a non-monotonic  $\Delta$ -dependence of  $\text{Im}[\varepsilon_\Delta]$  [see Fig. 3(b)]; the localization length, on the other hand, reduces monotonically with  $\Delta$ .

Another interesting question about the defect state is how it evolves from the underlying Hermitian system as  $\gamma$  increases and the flat band is formed. As Figs. 4(a) and (b) show, the defect state originates from the middle of the Hermitian band, especially when  $\Delta$  is small. By inspecting Eq. (5), we find that  $|\Delta| = t$  is a special case, where a  $\mathcal{PT}$  transition takes place at  $\gamma = t$ . We note that this is a different  $\mathcal{PT}$  transition from those that take place on the real- $\varepsilon$  axis when the flat band is formed. We also note that Eq. (5) applies only when the defect state is

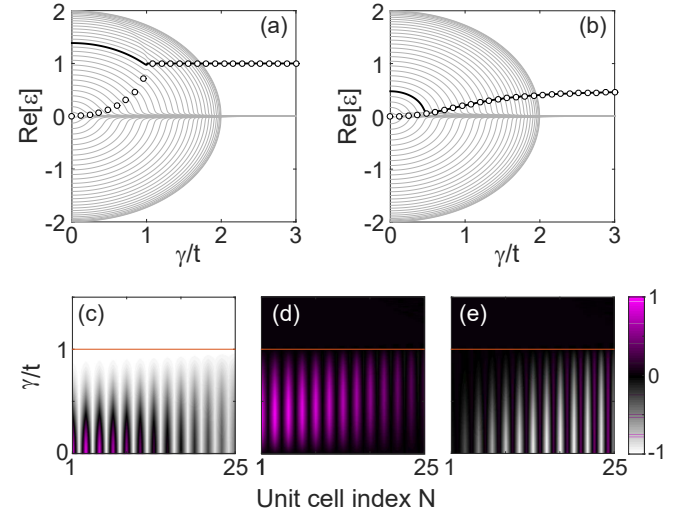


FIG. 4. (Color online) Emergence of a defect state from a non-Hermitian flat band as a function of the gain and loss strength  $\gamma$  with period  $m = 2$ . (a) and (b) Real part of all the modes in the system (solid lines) with  $\Delta = t$  and  $t/2$ , respectively. The black line indicates the evolution of the defect mode, and the circles are the prediction of Eq. (5). (c)–(e) False color plots of the pseudo-spin  $\langle\sigma\rangle_{x,y,z}$  as a function of position and  $\gamma$  in (a). Only the left 25 unit cells are shown.

localized and has a staggering intensity profile. Therefore, it is not surprising that its prediction in Fig. 4(a) [and Fig. 4(b)] deviates from the numerical result when  $\gamma$  is small and the defect state is still in the bulk. Nevertheless, the  $\mathcal{PT}$ -broken phase of  $\varepsilon_\Delta$  in  $\gamma > t$ , characterized by its  $\gamma$ -independent real part, is faithfully manifested by the numerical data.

Now if we inspect the spatial profile of the defect state as it evolves with  $\gamma$ , we observe an unconventional alignment of a pseudo-spin under the influence of a complex magnetic field. To be more specific, we first rewrite the effective Hamiltonian (2) using the Pauli matrices:

$$H_2 = t(1 + \cos ka) \sigma_x - t \sin ka \sigma_y + i\gamma \sigma_z \equiv -\mathbf{h} \cdot \boldsymbol{\sigma}, \quad (8)$$

where  $\mathbf{h}(\gamma) = [-t(1 + \cos ka), t \sin ka, -i\gamma]$  is our complex-valued pseudo-magnetic field. We normalized the wave function  $[\Psi_L, \Psi_G]^T$  in each unit cell when calculating  $\langle \boldsymbol{\sigma} \rangle$ , and the result is plotted in Figs. 4(c)–(e) as a function of  $\gamma$  when  $\Delta = t$ . It is clear that  $\langle \boldsymbol{\sigma} \rangle$  displays a spatially dependent orientation when  $\gamma < t$ , but an aligned  $\langle \boldsymbol{\sigma} \rangle$  is found across the whole lattice when  $\gamma > t$ . This value of  $\langle \boldsymbol{\sigma} \rangle$  is given by  $(-1, 0, 0)$  and can be viewed as the result of an unconventional alignment of a pseudo-spin, since the direction of a complex  $\mathbf{h}$  cannot be uniquely defined. The same alignment process takes place for other values of  $\Delta$  as well. For example,  $\langle \boldsymbol{\sigma} \rangle$  becomes  $(-0.8, 0, -0.6)$  when  $\Delta = t/2$ . We note that  $\langle \sigma_y \rangle$  is always zero in the aligned state; it is in fact proportional to the optical flux between the gain and loss sites in a unit cell by definition [i.e.,  $i(\Psi_G^* \Psi_L - \Psi_G \Psi_L^*)$ ], which vanishes as one can show that  $\Psi_L/\Psi_G = -\Delta/t$  is real (whose square gives  $R$ ).

**Conclusion and Discussion** — In summary, we have shown that NHPH symmetry can lead to a flat band consisting of photonic zero modes, which explains the previous finding in  $\mathcal{PT}$ -symmetric systems where NHPH symmetry is hidden. The defect states emerging from this flat band exhibit several interesting properties, such as possessing two types of links, one rigid within a unit cell and one soft between unit cells, as the defect states become increasingly localized with the non-Hermitian parameter. Their emergence can be viewed as an unconventional alignment of a pseudo-spin under the influence of a complex magnetic field, and in certain cases, the result of a  $\mathcal{PT}$  transition.

To introduce the point defect, one convenient way is to create a mirror plane, as we show in Fig. 5(a) for the  $m = 2$  case: the even-parity modes of the system have an effective detuning of  $t'$  at the lattice sites right next to the mirror plane, where  $t'$  is the coupling coefficient between the two halves of the system. Likewise, the odd-parity modes acquire an effective detuning of  $-t'$ . As a result, the defect states we have discussed now appear in pairs, one above the flat band and one below. They are NHPH-symmetric partners satisfying  $\varepsilon_{\Delta+} = -\varepsilon_{\Delta-}^*$ , and they have an identical intensity profile and hence the same localization length. The latter can be controlled either by

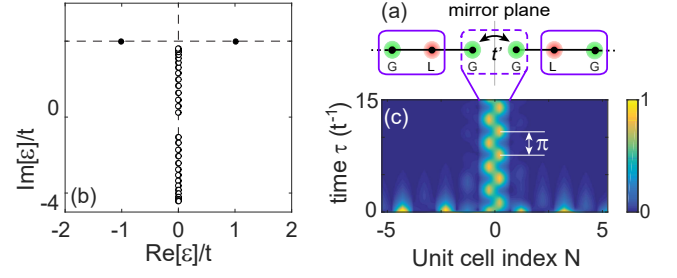


FIG. 5. (Color online) (a) Schematic of a symmetric setup with a non-Hermitian flat band. (b) Its spectrum at the laser threshold when  $t' = t$ ,  $\kappa = 2.2t$  and  $\gamma = 2.02t$ . The gain at the two central sites are 20% stronger than the rest. The filled and open dots show the defect states and the bulk states in the perturbed flat band, respectively. (c) Temporal evolution of the laser at its threshold with an initial random noise.

the non-Hermitian parameter  $\gamma$  (i.e., how strong the gain and/or loss modulation is) or the effective detuning  $\pm t'$  via the distance between the two halves.

To observe these defect states, one approach is to bring them to their lasing threshold ( $\text{Im}[\varepsilon] = 0$ ). In this setup we need to consider the intrinsic optical loss and absorption on each lattice site, and we take them to be uniform, represented by  $-i\kappa$  on the diagonal of the effective Hamiltonian. There is one issue here though: because the defect states feel a stronger loss than the bulk states that reside mostly on the gain sublattice, the latter will reach their lasing thresholds before the defect states. Take the case shown in Fig. 3(b) for example, there are bulk states with  $\text{Im}[\varepsilon] \approx \gamma > \text{Im}[\varepsilon_\Delta]$ . To overcome this issue, we introduce a non-Hermitian defect, e.g., by making  $\Delta$  complex and having a stronger gain. One example is shown in Fig. 5(b), where the pair of defect states in this symmetric setup indeed reach their lasing threshold before the bulk states. Assuming an inhomogeneous gain medium that supports both defect states, we can observe the blinking of the laser as a result of the beating between these two defect states, with a period given by  $\tau = \pi/\text{Re}[\varepsilon_\Delta]$  [see Fig. 5(c)].

\* li.ge@csi.cuny.edu

- [1] V. Apaja, M. Hyrkäs, and M. Manninen, Phys. Rev. A **82**, 041402(R) (2010).
- [2] M. Hyrkäs, V. Apaja, and M. Manninen, Phys. Rev. A **87**, 023614 (2013).
- [3] M. C. Rechtsman, J. M. Zeuner, A. Tünnermann, S. Nolte, M. Segev, and A. Szameit, Nature Photon. **7**, 153 (2013).
- [4] R. A. Vicencio, C. Cantillano, L. Morales-Inostroza, B. Real, C. Mejía-Cortés, S. Weimann, A. Szameit, and M. I. Molina, Phys. Rev. Lett. **114**, 245503 (2015).
- [5] S. Mukherjee, A. Spracklen, D. Choudhury, N. Goldman, P. Öhberg, E. Andersson, and R. R. Thomson, Phys. Rev. Lett. **114**, 245504 (2015).
- [6] M. Biondi, E. P. L. van Nieuwenburg, G. Blatter, S. D. Huber, and S. Schmidt, Phys. Rev. Lett. **115**, 143601 (2015).

- (2015).
- [7] C. L. Kane and E. J. Mele, Phys. Rev. Lett. **78**, 1932 (1997).
  - [8] F. Guinea, M. I. Katsnelson, and A. K. Geim, Nature Phys. **6**, 30 (2010).
  - [9] A. Simon, Angew. Chem. **109**, 1873 (1997).
  - [10] S. Deng, A. Simon, and J. Köhler, Angew. Chem. **110**, 664 (1998).
  - [11] S. Deng, A. Simon, and J. Köhler, J. Solid State Chem. **176**, 412 (2003).
  - [12] M. Imada and M. Kohno, Phys. Rev. Lett. **84**, 143(2000).
  - [13] E. Tang, J-W. Mei, and X-G. Wen, Phys. Rev. Lett. **106**, 236802 (2011).
  - [14] T. Neupert, L. Santos, C. Chamon, and C. Mudry, Phys. Rev. Lett. **106**, 236804 (2011).
  - [15] S. Yang, Z.-C. Gu, K. Sun, and S. Das Sarma, Phys. Rev. B **86**, 241112(R) (2012).
  - [16] T. Jacqumin et al., Phys. Rev. Lett. **112**, 116402 (2014).
  - [17] F. Baboux et al., Phys. Rev. Lett. **116**, 066402 (2016).
  - [18] J. T. Chalker, T. S. Pickles, and P. Shukla, Phys. Rev. B **82**, 104209 (2010).
  - [19] J. D. Bodyfelt, D. Leykam, C. Danieli, X. Yu, and S. Flach, Phys. Rev. Lett. **113**, 236403 (2014).
  - [20] D. Leykam, S. Flach, O. Bahat-Treidel, and A. S. Desyatnikov, Phys. Rev. B **88**, 224203 (2013).
  - [21] S. Flach, D. Leykam, J. D. Bodyfelt, P. Matthies, and A. S. Desyatnikov, Europhys. Lett. **105**, 30001 (2014).
  - [22] L. Ge, Ann. d. Phys., in press (2017).
  - [23] L. Ge, Phys. Rev. A **92**, 052103 (2015).
  - [24] G.-W. Chern and A. Saxena, Opt. Lett. **40**, 5806 (2014).
  - [25] M. I. Molina, Phys. Rev. A **92**, 063813 (2015).
  - [26] C. M. Bender and S. Boettcher, Phys. Rev. Lett. **80**, 5243 (1998).
  - [27] C. M. Bender, S. Boettcher, and P. N. Meisinger, J. Math. Phys. **40**, 2201 (1999).
  - [28] C. M. Bender, D. C. Brody, and H. F. Jones, Phys. Rev. Lett. **89**, 270401 (2002).
  - [29] R. El-Ganainy, K. G. Makris, D. N. Christodoulides, and Z. H. Musslimani, Opt. Lett. **32**, 2632 (2007).
  - [30] S. Klaiman, U. Gunther, and N. Moiseyev, Phys. Rev. Lett. **101**, 080402 (2008).
  - [31] Z. H. Musslimani, K. G. Makris, R. El-Ganainy, D. N. Christodoulides, Phys. Rev. Lett. **100**, 030402 (2008).
  - [32] K. G. Makris, R. El-Ganainy, D. N. Christodoulides, and Z. H. Musslimani, Phys. Rev. Lett. **100**, 103904 (2008).
  - [33] A. Guo, G. J. Salamo, D. Duchesne, R. Morandotti, M. Volatier-Ravat, V. Aimez, G. A. Siviloglou, and D. N. Christodoulides, Phys. Rev. Lett. **103**, 093902 (2009).
  - [34] A. Mostafazadeh, Phys. Rev. Lett. **102**, 220402 (2009).
  - [35] T. Kottos, Nature Phys. **6**, 166 (2010).
  - [36] S. Longhi, Phys. Rev. A **82**, 031801(R) (2010).
  - [37] Y. D. Chong, L. Ge, and A. D. Stone, Phys. Rev. Lett. **106**, 093902 (2011).
  - [38] P. Ambichl, K. G. Makris, L. Ge, Y. Chong, A. D. Stone, and S. Rotter, Phys. Rev. X **3**, 041030 (2013).
  - [39] L. Ge, Y. D. Chong, and A. D. Stone, Phys. Rev. A **85**, 023802 (2012).
  - [40] L. Ge, K. G. Makris, D. N. Christodoulides, and L. Feng, Phys. Rev. A **92**, 062135 (2015).
  - [41] L. Ge and A. D. Stone, Phys. Rev. X **4**, 031011 (2014).
  - [42] L. Ge and R. El-Ganainy, Sci. Rep. **6**, 24889 (2016).
  - [43] Z. Lin, H. Ramezani, T. Eichelkraut, T. Kottos, H. Cao, and D. N. Christodoulides, Phys. Rev. Lett. **106**, 213901 (2011).
  - [44] C. E. Rüter, K. G. Makris, R. El-Ganainy, D. N. Christodoulides, M. Segev, and D. Kip, Nature Phys. **6**, 192 (2010).
  - [45] A. Regensburger, C. Bersch, M. A. Miri, G. Onishchukov, D. N. Christodoulides, and U. Peschel, Nature (London) **488**, 167 (2012).
  - [46] S. Bittner, B. Dietz, U. Günther, H. L. Harney, M. Miski-Oglu, A. Richter, and F. Schäfer, Phys. Rev. Lett. **108**, 024101 (2012).
  - [47] L. Feng, Y.-L. Xu, W. S. Fegadolli, M.-H. Lu, J. E. B. Oliveira, V. R. Almeida, Y.-F. Chen, and A. Scherer, Nature Mater. **12**, 108 (2013).
  - [48] L. Feng, Z. J. Wong, R.-M. Ma, Y. Wang, and X. Zhang, Science **346**, 972 (2014).
  - [49] H. Hodaei, M. A. Miri, M. Heinrich, D. N. Christodoulides, and M. Khajavikhan, Science **346**, 975 (2014).
  - [50] B. Peng et al., Nature Phys. **10**, 394 (2014).
  - [51] L. Chang et al., Nature Photon. **8**, 524 (2014).
  - [52] B. Zhu, R. Lü, and S. Chen, Phys. Rev. A **89**, 062102 (2014).
  - [53] H. Zhao, S. Longhi, and L. Feng, Sci. Rep. **5**, 17022 (2015).
  - [54] S. Malzard, C. Poli, and H. Schomerus, Phys. Rev. Lett. **115**, 200402 (2015).
  - [55] L. Ge, Phys. Rev. A **95**, 023812 (2017).
  - [56] J. Alicea, Rep. Prog. Phys. **75**, 076501 (2012).
  - [57] C. W. J. Beenakker, Rev. Mod. Phys. **87**, 1037 (2015).
  - [58] S. D. Sarma, M. Freedman, and C. Nayak, npj Quantum Information **1**, 15001 (2015).
  - [59] W. P. Su, J. R. Schrieffer, and A. J. Heeger, Phys. Rev. Lett. **42**, 1698 (1979).
  - [60] H. Schomerus, Opt. Lett. **38**, 1912 (2013).